Midgap edge states and pairing symmetry of quasi-one-dimensional organic superconductors

K. Sengupta, Igor Žutić, Hyok-Jon Kwon, Victor M. Yakovenko, and S. Das Sarma
Department of Physics and Center for Superconductivity, University of Maryland, College Park, Maryland 20742-4111
(Received 15 October 2000; published 23 March 2001)

The singlets *s*- and *d*-, and triplet *p*-wave pairing symmetries in quasi-one-dimensional organic superconductors can be experimentally discriminated by probing the Andreev bound states at the sample edges. These states have the energy in the middle of the superconducting gap and manifest themselves as a zero-bias peak in tunneling conductance into the corresponding edge. Their existence is related to the sign change of the pairing potential around the Fermi surface. We present an exact self-consistent solution of the edge problem showing the presence of the midgap states for p_x-wave superconductivity. The spins of the edge state respond paramagnetically to a magnetic field parallel to the vector **d** that characterizes triplet pairing.

DOI: 10.1103/PhysRevB.63.144531 PACS number(s): 74.70.Kn, 73.20.−r, 74.50.+r

I. INTRODUCTION

Quasi-one-dimensional (Q1D) conductors of the tetramethyltetraselenafulvalene $(TMTSF)_2X$ family[1] (the Bechgaard salts) are the first organic materials where superconductivity was discovered twenty years ago with $T_c \approx 1$ K.[2] Abrikosov proposed that the superconductivity is *p*-wave triplet,[3] because it is suppressed by nonmagnetic impurities.[4] Gor'kov and Jérome observed that the upper critical magnetic field H_{c2} exceeds the Pauli paramagnetic limit, which is also a signature of triplet superconductivity.[5] Recent data show that H_{c2} exceeds the Pauli limit by a factor greater than 4.[6] Another signature of triplet pairing is that the Knight shift does not change between the normal and superconducting states.[7] However, the temperature dependence of the NMR relaxation rate[8] and analogy with the high-temperature superconductors led to an alternative proposal of the *d*-wave symmetry.[9] It was also proposed that a singlet Q1D superconductivity can overcome the Pauli paramagnetic limit by forming the spatially nonuniform Larkin-Ovchinnikov-Fulde-Ferrell state.[10] However, the quantitative analysis of the experimental data[6] by Lebed *et al.*[11,12] did not support this proposal and favored triplet pairing. The *f* wave[13] was also proposed recently. So the pairing symmetry in the Bechgaard salts remains hotly debated.

In this paper, we propose a phase-sensitive method to distinguish experimentally between the *s*-, *p*-, and *d*-wave symmetries. We employ a relation between sign change of the superconducting pair potential around the Fermi surface and existence of the surface Andreev bound states, discovered for *p* wave by Buchholtz and Zwicknagl[14] and for *d* wave by Hu.[15] For different superconducting symmetries, we determine which edges of $(TMTSF)_2X$ must have the Andreev bound states. The energy of these states is in the middle of the superconducting gap, thus they can be observed in tunneling experiments as zero-bias conductance peaks.[14,16,17] We also obtain an exact self-consistent solution of the edge problem for a p_x-wave Q1D superconductor by mapping it onto the kink soliton solution for a one-dimensional (1D) charge-density wave.[18] We show that the spins of the edge states should exhibit a strong paramagnetic response to a magnetic field parallel to the polarization vector **d** of the triplet pairing and propose the corresponding experiment. All calculations are performed at zero temperature.

II. Q1D SUPERCONDUCTIVITY

Classification of superconducting pairing symmetry is particularly simple for a 1D electron gas. Its Fermi surface consists of two points $\pm k_F$. Let us introduce the operators $\hat{\psi}^\alpha_\sigma$ of the right ($\alpha=R$) and left ($\alpha=L$) moving electrons with the momenta close to $\pm k_F$ and the spin $\sigma=\uparrow,\downarrow$. The Cooper pairing can be either singlet $\langle \hat{\psi}^\alpha_\sigma \hat{\psi}^{\bar{\alpha}}_{\sigma'} \rangle \propto \epsilon_{\sigma\sigma'}\Delta^\alpha = i\hat{\sigma}^{(y)}_{\sigma\sigma'}\Delta^\alpha$ or triplet $\langle \hat{\psi}^\alpha_\sigma \hat{\psi}^{\bar{\alpha}}_{\sigma'} \rangle \propto i\hat{\sigma}^{(y)}(\mathbf{d}\cdot\hat{\boldsymbol{\sigma}})\Delta^\alpha$. Here $\bar{\alpha}=L,R$ for $\alpha=R,L$; $\epsilon_{\sigma\sigma'}$ is the antisymmetric metric tensor, and $\hat{\boldsymbol{\sigma}}$ are the Pauli matrices acting in the spin space; **d** is a unit vector of polarization of the triplet state. Since the fermion operators anticommute, the superconducting pair potential has either the same ($\Delta^R=\Delta^L$) or the opposite ($\Delta^R=-\Delta^L$) signs at the two Fermi points for the singlet or triplet pairing.

The real $(TMTSF)_2X$ materials are three-dimensional (3D) crystals consisting of parallel chains. In the tight-binding approximation, the electron energy dispersion (measured from the Fermi energy) can be written as[19]

$$\epsilon(\mathbf{k}) = v_F(|k_x|-k_F) - 2t_b\cos(k_y b) - 2t_c\cos(k_z c). \quad (1)$$

In the right-hand side of Eq. (1), the first term represents the dispersion along the chains, linearized near the Fermi energy with a Fermi velocity v_F. The two other terms describe electron tunneling between the chains in the *y* and *z* directions with the amplitudes t_b and t_c. $\mathbf{k}=(k_x,k_y,k_z)$ is the 3D electron momentum, *b* and *c* are the lattice spacings in the *y* and *z* directions, and $\hbar=1$.

The Fermi surface corresponding to Eq. (1) consists of two disconnected sheets, sketched in Fig. 1 with a greatly exaggerated warping in the k_y direction. In the simplest case, the superconducting pair potential $\Delta(\mathbf{k})$ is equal to a constant Δ^α on a given sheet α of the Fermi surface, and $\Delta^R=\pm\Delta^L$ for the singlet or triplet pairing, respectively. In both cases, the superconducting gap has no nodes on the Fermi

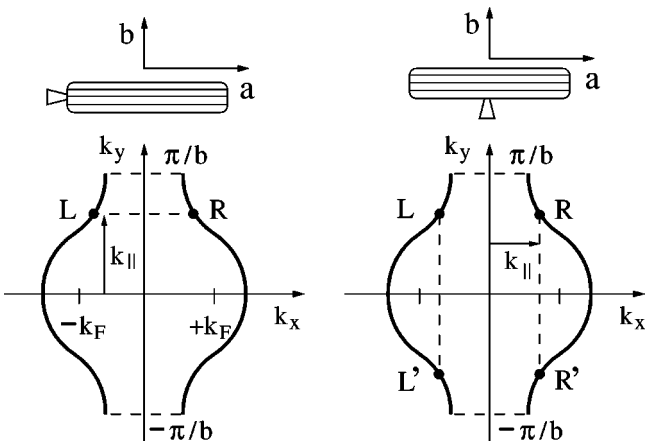

FIG. 1. Top: $(TMTSF)_2X$ samples with the lines indicating 1D chains. The left and right panels sketch tunneling along the *a* and *b* axes. Bottom: The Fermi surface of $(TMTSF)_2X$, sketched with a greatly exaggerated warping in the k_y direction. Reflection from the edge perpendicular (parallel) to the chains changes electron momentum from L to R (R' to R and L' to L), as shown in the left (right) panel.

surface. These two symmetries can be called *s* and p_x waves. Other symmetries will be discussed at the end of the paper (see Fig. 3).

Electron eigenstates of the energies E_n are described in a superconductor by the Bogolyubov-de Gennes (BdG) wave functions $\Psi_n = e^{i\mathbf{r}\cdot\mathbf{k}_F}[u_{n,\sigma}(x), \epsilon_{\sigma'\bar{\sigma}'} v_n^{\bar{\sigma}'}(x)]$, where $u_{n,\sigma}$ and $v_n^{\bar{\sigma}'}$ are the electronlike and holelike components with the spins σ and $\bar{\sigma}'$, and $\bar{\sigma}' = \downarrow, \uparrow$ is the spin index opposite to $\sigma' = \uparrow, \downarrow$. The 3D Fermi momenta $\mathbf{k}_F$ belong to the warped Fermi surface shown in Fig. 1. Near the Fermi surface α, the wave functions satisfy the linearized BdG equation[20,21]

$$\begin{pmatrix} -i\alpha v_F \partial_x & (\hat{\boldsymbol{\sigma}}\cdot\mathbf{d})\Delta^{\alpha}(x) \\ (\hat{\boldsymbol{\sigma}}\cdot\mathbf{d})\Delta^{\alpha *}(x) & i\alpha v_F \partial_x \end{pmatrix} \begin{pmatrix} u_n^{\alpha} \\ v_n^{\alpha} \end{pmatrix} = E_n \begin{pmatrix} u_n^{\alpha} \\ v_n^{\alpha} \end{pmatrix}, \quad (2)$$

where $\alpha v_F = \pm v_F$ for $\alpha = R, L$. The term $(\hat{\boldsymbol{\sigma}}\cdot\mathbf{d})$ is present for triplet superconductivity and absent for the singlet one. It operates on the spin indices of the components u and v.

In general, the vector $\mathbf{d}$ is a function of the position on the Fermi surface, e.g., in ^{3}He-*A* and ^{3}He-*B*.[22] The quantitative analysis[12] of the experimental data[6] gives the following information about the components of the vector $\mathbf{d}$ in the $(TMTSF)_2X$ crystal: $d_a \neq 0$, $d_b = 0$, and d_c is unknown. In this paper, we make the simplest assumption that $\mathbf{d}$ is a real vector pointing along the *a* axis parallel to the chains (the so-called polar state[22]). If we select the spin-quantization axis along $\mathbf{d}$, then the 4×4 matrix Eq. (2) decouples into two 2×2 matrix equations for the wave functions $(u_\sigma, \epsilon_{\sigma\bar{\sigma}} v^{\bar{\sigma}})$

$$\begin{pmatrix} -i\alpha v_F \partial_x & \sigma\Delta^{\alpha}(x) \\ \sigma\Delta^{\alpha *}(x) & i\alpha v_F \partial_x \end{pmatrix} \begin{pmatrix} u_{n,\sigma}^{\alpha} \\ \sigma v_n^{\alpha,\bar{\sigma}} \end{pmatrix} = E_n \begin{pmatrix} u_{n,\sigma}^{\alpha} \\ \sigma v_n^{\alpha,\bar{\sigma}} \end{pmatrix}. \quad (3)$$

Here the index $\sigma = \uparrow, \downarrow$ takes the values $\pm$ when used as a coefficient. It is present in the off-diagonal term $\sigma\Delta^{\alpha}$ only for triplet, but not for singlet pairing. To simplify equations, we omit the spin index σ in Secs. III and IV and restore it in Sec. V. Notice that Eqs. (2) and (3) depend only on the 1D coordinate *x*, because the 3D dispersion (1) in k_y and k_z has been absorbed into the definition of the 3D Fermi momenta $\mathbf{k}_F$.

III. EDGE STATES

Let us consider a system occupying the semi-infinite space $x \geqslant 0$ with an impenetrable edge at $x = 0$. When the electron reflects from the edge specularly, its k_x momentum changes sign, whereas the other components remain the same. The electron scatters from the point $\mathbf{k}_F^L$ at the left sheet of the Fermi surface to the point $\mathbf{k}_F^R$ at the right sheet, as shown in the left panel of Fig. 1. Thus, its BdG wave function Ψ is a superposition of the *R* and *L* terms

$$\Psi = \frac{1}{\sqrt{2}} \left[e^{i\mathbf{r}\cdot\mathbf{k}_F^R} \begin{pmatrix} u_n^R(x) \\ v_n^R(x) \end{pmatrix} - e^{i\mathbf{r}\cdot\mathbf{k}_F^L} \begin{pmatrix} u_n^L(x) \\ v_n^L(x) \end{pmatrix} \right]. \quad (4)$$

We have selected the minus sign in Eq. (4) so that the impenetrable boundary condition $\Psi(x=0) = 0$ gives

$$u^R(0) = u^L(0), \quad v^R(0) = v^L(0). \quad (5)$$

First let us use a step-function approximation for the pairing potential $|\Delta^{\alpha}(x)| = \Delta_0 \theta(x)$. Then, the plane waves $[u^{\alpha}(x), v^{\alpha}(x)] \propto e^{ik_x x}$ are the eigenfunctions of Eq. (3) with the energies $E = \pm\sqrt{(v_F k_x)^2 + \Delta_0^2}$. However, the energy is real also when k_x is imaginary (but not a combination of real and imaginary parts) $k_x = i\kappa$ and $E = \pm\sqrt{\Delta_0^2 - (v_F\kappa)^2}$. For $\kappa > 0$, this solution describes an electron eigenfunction localized near the edge at $x = 0$ $[u^{\alpha}(x), v^{\alpha}(x)] \propto e^{-\kappa x}$. Because $u^{\alpha}/v^{\alpha} = \Delta^{\alpha}/(\alpha i v_F \kappa + E)$, the boundary condition (5) can be satisfied only for p_x wave with $\Delta^R = -\Delta^L$, but not for *s* wave with $\Delta^R = \Delta^L$. Thus, in the p_x case, there is an edge electron state with the energy in the middle of the superconducting gap $E = 0$, and the localization length is equal to the coherence length $1/\kappa = v_F/\Delta_0$.

The step-function approximation does not take into account the BdG self-consistency condition $\Delta^{\alpha}(x) = g\Sigma_n u_n^{\alpha}(x) v_n^{\alpha *}(x)$, where g is the effective coupling constant,[23] and the sum is taken over all occupied states with $E_n < 0$ (at zero temperature). To solve the problem, let us extend the wave function (4) from the positive semispace $x > 0$ to the full space $-\infty < x < \infty$. Let us define $[u(x), v(x)] = [u^R(x), v^R(x)]$ and $\Delta(x) = \Delta^R(x)$ for $x > 0$, and $[u(x), v(x)] = [u^L(-x), v^L(-x)]$ and $\Delta(x) = \Delta^L(-x)$ for $x < 0$. Because of the boundary condition (5), the wave function $[u(x), v(x)]$ is continuous at $x = 0$ and satisfies a single BdG equation for $-\infty < x < \infty$ with the BdG self-consistency condition

$$\begin{pmatrix} -iv_F \partial_x & \Delta(x) \\ \Delta^*(x) & +iv_F \partial_x \end{pmatrix} \begin{pmatrix} u_n(x) \\ v_n(x) \end{pmatrix} = E_n \begin{pmatrix} u_n(x) \\ v_n(x) \end{pmatrix}, \quad (6)$$

$$\Delta(x) = g \sum_n u_n(x) v_n^*(x). \quad (7)$$

Equations (6) and (7) coincide with the exactly solvable equations describing 1D charge-density wave in polyacetylene.[18] The p_x-wave problem, where $\Delta(x)$ changes sign, $\Delta(+\infty)=-\Delta(-\infty)$, maps onto the kink soliton solution[18]

$$\Delta(x)=i\Delta_0\tanh(\kappa x); \tag{8}$$

$$E_0=0, \quad \begin{pmatrix} u_0(x) \\ v_0(x) \end{pmatrix}=\frac{\sqrt{\kappa}}{2\cosh(\kappa x)}\begin{pmatrix} 1 \\ -1 \end{pmatrix}; \tag{9}$$

$$E_k=\pm\sqrt{v_F^2k^2+\Delta_0^2}, \tag{10}$$

$$\begin{pmatrix} u_k(x) \\ v_k(x) \end{pmatrix}=\frac{e^{ikx}}{2E_k\sqrt{L_x}}\begin{pmatrix} E_k+v_Fk+\Delta(x) \\ E_k-v_Fk-\Delta(x) \end{pmatrix}, \tag{11}$$

where L_x is the length of the sample along the chains. One can check explicitly that solutions (8)–(11) satisfy Eqs. (6) and (7).[24] They also have the property of supersymmetry.[25] The localized electron state (9) with $E_0=0$ corresponds to the Andreev edge state in the p_x-wave superconductor. In the s-wave case, where $\Delta(x)$ does not change sign: $\Delta(+\infty)=\Delta(-\infty)$, the solution of Eqs. (6) and (7) gives a uniform $\Delta(x)$, which does not have bound states. The existence of the midgap state in the case where $\Delta(x)$ changes sign is guaranteed by the index theorem and does not depend on the detailed functional form of the pair potential.[26]

BdG states are described by the operators $\hat{\Psi}=u\hat{\psi}+v^*\hat{\psi}^\dagger$. The expectation value of electric charge ρ in the edge states is zero $\rho\propto|u_0|^2-|v_0|^2=0$. For a 1D p_x-wave superconductor with only one species of spin, Eqs. (4) and (9) imply that the two edge states at the opposite ends are described by the Majorana operators of the opposite parity $\hat{\Psi}^\dagger=\pm\hat{\Psi}$.[27] There was a proposal to use such edge Majorana fermions for quantum computing.[27] However, in a Q1D p_x-wave superconductor, the midgap states with different momenta $\mathbf{k}_\parallel$ parallel to the edge and spins σ form a degenerate continuum with $\hat{\Psi}^\dagger_{\mathbf{k}_\parallel,\sigma}=\pm\hat{\Psi}_{-\mathbf{k}_\parallel,\sigma}$.[28]

IV. TUNNELING

Let us consider electron tunneling between the superconducting $(TMTSF)_2X$ and a normal metallic tip. The tunneling junction can be modeled as two semi-infinite regions, normal (N) and superconducting (S), with a flat interface between them. Following Refs. 16, 29, and 30, we solve the BdG equations in the ballistic regime assuming specular reflection and the translational invariance parallel to the interface.[31] To make the problem analytically tractable, we use the step-function approximation for the pair potential. At the interface, we impose the boundary conditions $\Psi_N=\Psi_S$ and $\hat{v}_N\Psi_N=\hat{v}_S\Psi_S+2i\mathcal{H}\Psi_N$,[32] where $\hat{v}_{N,S}$ are the components of the velocity operators perpendicular to the interface in metal and superconductor, and $\mathcal{H}$ is the strength of the interface barrier. From the solution of the BdG equations, we find the probabilities $B(E,\mathbf{k}_\parallel)$ and $A(E,\mathbf{k}_\parallel)$ of the normal and Andreev[21] reflections as functions of the electron energy E and momentum $\mathbf{k}_\parallel$ parallel to the interface. They determine the dimensionless conductance $G=1+A-B$ in the formula for the electric current through the contact[29]

$$I=\frac{2eS}{h}\int\frac{d^2k_\parallel dE}{(2\pi)^2}[f(E-eV)-f(E)]G(E,\mathbf{k}_\parallel). \tag{12}$$

Here S is the contact area, V the bias voltage, $f(E)$ the Fermi function, e the electron charge, and h the Planck constant. It follows from Eq. (12) that the differential conductance of the contact at zero temperature,

$$\overline{G}(V)=\frac{dI}{dV}=\frac{2e^2S}{h}\int\frac{d^2k_\parallel}{(2\pi)^2}G(eV,\mathbf{k}_\parallel), \tag{13}$$

is proportional to the average over $\mathbf{k}_\parallel$ of the dimensionless conductance G.[33] The latter is determined by the transmission coefficient T at a given $\mathbf{k}_\parallel$ (Refs. 16 and 32)

$$G_\pm=T\frac{1+T|\Gamma|^2+(T-1)|\Gamma|^4}{|1\pm(T-1)\Gamma^2|^2}, \tag{14}$$

where

$$\Gamma(E)=\begin{cases}[E-\mathrm{sgn}(E)\sqrt{E^2-\Delta_0^2}]/\Delta_0, & |E|\geqslant\Delta_0, \\ (E-i\sqrt{\Delta_0^2-E^2})/\Delta_0, & |E|\leqslant\Delta_0,\end{cases} \tag{15}$$

$$T=4v_Nv_S/[(v_N+v_S)^2+4\mathcal{H}^2]. \tag{16}$$

The $\pm$ sign in Eq. (14) is the relative sign of the pair potentials for the two branches of BdG quasiparticles involved in tunneling. For tunneling along the chains, the two branches correspond to the points L and R in the left panel of Fig. 1, and the sign in Eq. (14) is $\mathrm{sgn}(\Delta^R\Delta^L)$, $+$ for s wave and $-$ for p_x wave. Averaging in Eq. (13) is performed taking into account that v_N and v_S in Eq. (16) and Δ_0 in Eq. (15) may depend on $\mathbf{k}_\parallel$.

As follows from Eq. (14), G_+ and G_- coincide for a fully transparent interface $(T=1)$ $G_+=G_-=1+|\Gamma|^2$.[29] However, typically $T<1$, both because of the barrier potential $\mathcal{H}$ and the mismatch of the normal Fermi velocities $v_N\neq v_S$ in metal and superconductor in Eq. (16).[32] At low interface transparency $T\ll1$, G_-, and G_+ behave as shown in the left and right panels of Fig. 2 for $T=0.5$ and $T=0.25$. Inside the energy gap, where $|\Gamma|=1$, $G_-(E)$ has a Lorentzian shape with the maximum of 2 at $E=0$, the width proportional to T, and the minimum proportional to T^2 at $|E|=\Delta_0$

$$G_-(E)=\frac{T^2/2(1-T)}{(E/\Delta_0)^2+T^2/4(1-T)}, \quad |E|\leqslant\Delta_0. \tag{17}$$

$G_+(E)$ shows the opposite behavior: a minimum proportional to T^2 at $E=0$ and the maxima of 2 at $|E|=\Delta_0$

$$G_+(E)=\frac{T^2/2(1-T)}{1-(E/\Delta_0)^2+T^2/4(1-T)}, \quad |E|\leqslant\Delta_0.$$

Both G_+ and G_- approach the normal-state conductance T at $|E|\gg\Delta_0$.

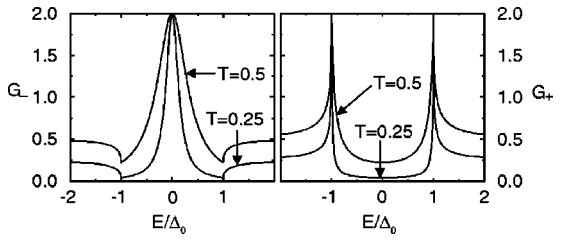

FIG. 2. Dimensionless conductances G_- (left panel) and G_+ (right panel) given by Eq. (14) are plotted versus energy E for the transmission coefficients $T=0.5$ and 0.25. G_+ and G_- correspond to the cases where the superconducting pairing potential has the same or the opposite signs for the two branches of BdG quasiparticles involved in tunneling (the points L and R, R', and R, L' and L in Fig. 1).

The zero-bias conductance peak (ZBCP), shown in the left panel of Fig. 2, is a manifestation of the midgap Andreev bound states. They exist at those edges where momentum reflection from the edge connects the points on the Fermi surface with opposite signs of the superconducting pair potential. As shown in the left and right panels of Fig. 1, reflection from the edge perpendicular to the chains connects L to R, and reflection from the edge parallel to the chains connects R' to R and L' to L. By comparing the signs of the pair potential at these points for the superconducting symmetries[12] listed in Table I and sketched in Fig. 3, we determine whether ZBCP must be present in tunneling into those edges. Comparison of Table I with the experiment should uncover the superconducting symmetry of $(TMTSF)_2X$.

V. SPIN RESPONSE

Now let us discuss the spin response of the edge states in a triplet superconductor subject to an external magnetic field **H**. (Here we do not consider orbital effects of the magnetic field, such as the Meissner effect.) In this case, the matrix in Eq. (2) should be replaced by the following matrix:

$$\begin{pmatrix} -i\alpha v_F\partial_x-\mu_B(\mathbf{H}\cdot\boldsymbol{\sigma}) & (\hat{\boldsymbol{\sigma}}\cdot\mathbf{d})\Delta^{\alpha}(x) \\ (\hat{\boldsymbol{\sigma}}\cdot\mathbf{d})\Delta^{\alpha *}(x) & i\alpha v_F\partial_x-\mu_B(\mathbf{H}\cdot\boldsymbol{\sigma}) \end{pmatrix}, \quad (18)$$

TABLE I. Presence (yes) or absence (no) of a zero-bias conductance peak in electron tunneling along the *a* and *b* axes (see the top left and right panels in Fig. 1) for different symmetries of the superconducting pairing potential $\Delta(\mathbf{k})$ (Refs. 34 and 35).

Symmetry	$\Delta(\mathbf{k})$	*a*-axis ZBCP	*b*-axis ZBCP
s	const	no	no
p_x	$\sin(k_x a)$	yes	no
p_y	$\sin(k_y b)$	no	yes
$d_{x^2-y^2}$	$\cos(k_y b)$	no	no
d_{xy}	$\sin(k_x a)\sin(k_y b)$	yes	yes

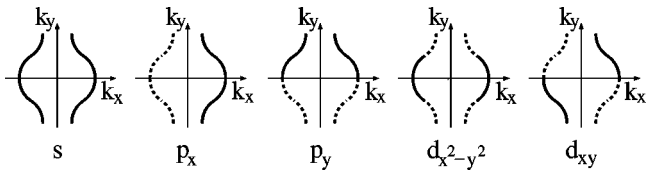

FIG. 3. Different symmetries of the pairing potential $\Delta(\mathbf{k})$ in a Q1D superconductor. The solid and dotted lines represent the portions of the Fermi surface with the opposite signs of the pairing potential.

where μ_B is the Bohr magneton, and the electron g factor is 2.

If $\mathbf{H}\|d$, then, by selecting the spin-quantization axis along **d**, the 4×4 matrix Eq. (18) is decoupled into two 2×2 matrix equations similar to Eq. (3) for the wave functions $(u_\sigma, \epsilon_{\sigma\sigma}\bar{v}^{\sigma})$ with the matrix

$$\begin{pmatrix} -i\alpha v_F\partial_x-\sigma\mu_B H & \sigma\Delta^{\alpha}(x) \\ \sigma\Delta^{\alpha *}(x) & i\alpha v_F\partial_x-\sigma\mu_B H \end{pmatrix}. \quad (19)$$

For a given spin projection σ, the magnetic field H enters Eq. (19) as a unity matrix and simply shifts the spectrum (9) and (10) by $-\sigma\mu_B H$. Thus, the energies of the up and down spin states become split by $\mp\mu_B H$, including the midgap state $E_0=\mp\mu_B H$. Because this state is half filled, the edge states with the spin parallel (antiparallel) to the magnetic field become completely occupied (empty). This generates spin $\hbar/2$ and magnetic moment μ_B at the end of each chain. Such a giant magnetic moment was predicted by Hu and Yan[15,36] for the edge states in a singlet *d*-wave superconductor. In a triplet superconductor, the effect is similar, but anisotropic.

Indeed, suppose now that $\mathbf{H}\perp d$. In this case, it is convenient to select the spin-quantization axis $\hat{z}$ along **H** and the $\hat{x}$ axis along **d**. Then Eq. (18) separates into two 2×2 matrix equations similar to Eq. (3) for the wave functions $(u_\sigma, \epsilon_{\sigma\sigma}\bar{v}^{\sigma})$ with the matrix

$$\begin{pmatrix} -i\alpha v_F\partial_x-\sigma\mu_B H & \Delta^{\alpha}(x) \\ \Delta^{\alpha *}(x) & i\alpha v_F\partial_x+\sigma\mu_B H \end{pmatrix}. \quad (20)$$

The magnetic field H can be eliminated from Eq. (20) by adjusting the Fermi momenta for the up and down spin states $k_{F,\sigma}=k_F+\sigma\mu_B H/v_F$. Thus, the energy spectrum of the system remains the same as in Eqs. (9) and (10). Particularly, the energy of the midgap state does not split, $E_0=0$, thus no unbalanced spin and magnetic moment are generated on the edge.

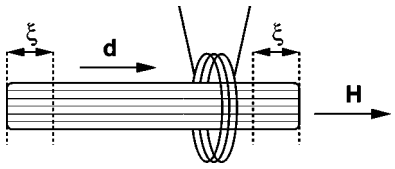

FIG. 4. Schematic experimental setup to measure magnetic susceptibility of the edge states localized at the ends of the chains.

We see that the edge spin response of a triplet superconductor is opposite to its bulk spin response. It is well known[22] that the bulk spin susceptibility for $\mathbf{H}\perp d$ is the same as in the normal state, whereas for $\mathbf{H}\|d$ it vanishes at zero temperature. For the edge states, the spin response vanishes for $\mathbf{H}\perp d$ and is paramagnetic for $\mathbf{H}\|d$. Nominally, the edge spin susceptibility is infinite, because, formally, an infinitesimal magnetic field can completely polarize the edge spins. We can only estimate the maximal magnetic moment, which is $\mu_B = 9.3\times 10^{-24}$ A m^2 per chain or $\mu_B/bc = 9\times 10^{-6}$ μA per unit area of the edge, where $b=0.77$ and $c=1.35$ nm.[19]

The generation of paramagnetic moments by the edge states for $\mathbf{H}\|d$ could be observed experimentally by measuring magnetic susceptibility with a coil as shown in Fig. 4, where we assume that **d** is directed along the chains. In the bulk, far from the edges, the susceptibility should be diamagnetic, because of the orbital Meissner effect[37] and vanishing spin bulk susceptibility for $\mathbf{H}\|d$. However, when the coil is moved toward the sample end, the susceptibility should change sign and become paramagnetic because of the edge states. They are localized within the coherence length $\xi = \hbar v_F/\Delta_0 = 0.6$ μm, where we used $\Delta_0 = 0.22$ meV, $v_F = t_a a/\sqrt{2}\hbar = 190$ km/s, $t_a = 0.25$ eV, and $a = 0.73$ nm.[19] The effect should depend on the coil orientation relative to the vector **d**. Therefore, this experiment could confirm the existence of the edge states and the pairing symmetry in the $(TMTSF)_2X$ superconductors.

VI. CONCLUSIONS

We have constructed an exact analytical self-consistent solution of the edge problem for a p_x-wave Q1D superconductor by mapping it onto the kink soliton solution for a 1D charge-density wave. The edge electron midgap states exist when the pairing potential has opposite signs at the different parts of the Fermi surface connected by momentum reflection from the edge. These states manifest themselves as zero-bias peaks in tunneling conductance. Thus, the pairing symmetry of the Q1D superconductors can be determined by tunneling into the edges perpendicular and parallel to the chains. The spins of the edge state respond paramagnetically to a magnetic field parallel to the vector **d** that characterizes triplet pairing, generating the magnetic moment μ_B per chain.

The $(TMTSF)_2X$ materials are expected to have electron edge states also in the magnetic-field-induced spin-density-wave phase, which exhibits the quantum Hall effect.[38] Those states are chiral and have dispersion inside the energy gap. The midgap states discussed in the present paper also acquire chiral dispersion due to the orbital effect of a magnetic field, similar to cuprates.[39] Another interesting example of the edge states in a 1D electron gas was studied theoretically in Ref. 40 for the Luther-Emery fermions in the bosonized representation.

Note added in proof. A more subtle consideration of the results of Sec. V shows that the spin of an edge state is actually fractional and is equal to $\hbar/4$ (per each end of each chain), not $\hbar/2$. Correspondingly, the magnetic moment is $\mu_B/2$, and the numerical estimates given in Sec. V should be multiplied by an additional factor 1/2. Derivation of these results will be given in a separate paper. The authors are grateful to A. Yu. Kitaev and D. A. Ivanov for very illuminating discussions of this subject.[41]

K.S., H.J.K., and V.M.Y. were supported by the Packard Foundation and NSF Grant No. DMR-9815094; I.Ž. and S.D.S. by the US-ONR and DARPA.

[1] X represents inorganic anions such as ClO_4 or PF_6.
[2] D. Jérome, A. Mazaud, M. Ribault, and K. Bechgaard, J. Phys. (France) Lett. **41**, L92 (1980).
[3] A. A. Abrikosov, J. Low Temp. Phys. **53**, 359 (1983).
[4] M.-Y. Choi *et al.*, Phys. Rev. B **25**, 6208 (1982); S. Bouffard *et al.*, J. Phys. C **15**, 2951 (1982); C. Coulon *et al.*, J. Phys. (France) **43**, 1721 (1982); S. Tomić *et al.*, J. Phys. (Paris), Colloq. **44**, C3-1075 (1983).
[5] L. P. Gor'kov and D. Jérome, J. Phys. (France) Lett. **46**, L643 (1985); L. I. Burlachkov, L. P. Gor'kov, and A. G. Lebed', Europhys. Lett. **4**, 941 (1987).
[6] I. J. Lee, M. J. Naughton, G. M. Danner, and P. M. Chaikin, Phys. Rev. Lett. **78**, 3555 (1997); I. J. Lee, P. M. Chaikin, and M. J. Naughton, Phys. Rev. B **62**, R14 669 (2000).
[7] I. J. Lee *et al.*, cond-mat/0001332 (unpublished).
[8] M. Takigawa, H. Yasuoka, and G. Saito, J. Phys. Soc. Jpn. **56**, 873 (1987).
[9] M. T. Beal-Monod, C. Bourbonnais, and V. J. Emery, Phys. Rev. B **34**, 7716 (1986); Y. Hasegawa and H. Fukuyama, J. Phys. Soc. Jpn. **56**, 877 (1987).
[10] N. Dupuis, G. Montambaux, and C. A. R. Sá de Melo, Phys. Rev. Lett. **70**, 2613 (1993); N. Dupuis and G. Montambaux, Phys. Rev. B **49**, 8993 (1994); N. Dupuis, *ibid.* **51**, 9074 (1995).
[11] A. G. Lebed, Phys. Rev. B **59**, R721 (1999).
[12] A. G. Lebed, K. Machida, and M. Ozaki, Phys. Rev. B **62**, R795 (1999).
[13] K. Kuroki, R. Arita, and H. Aoki, Phys. Rev. B **63**, 094509 (2001).
[14] L. J. Buchholtz and G. Zwicknagl, Phys. Rev. B **23**, 5788 (1981).
[15] C.-R. Hu, Phys. Rev. Lett. **72**, 1526 (1994); J. Yang and C.-R. Hu, Phys. Rev. B **50**, 16 766 (1994).
[16] Y. Tanaka and S. Kashiwaya, Phys. Rev. Lett. **74**, 3451 (1995); S. Kashiwaya, Y. Tanaka, M. Koyanagi, and K. Kajimura, Phys. Rev. B **53**, 2667 (1996).
[17] J. Y. T. Wei *et al.*, Phys. Rev. Lett. **81**, 2542 (1998); I. Iguchi *et al.*, Phys. Rev. B **62**, R6131 (2000).
[18] S. A. Brazovskii, Zh. Eskp. Teor. Fiz. **78**, 677 (1980) [Sov. Phys. JETP **51**, 342 (1980)]; H. Takayama, Y. R. Lin-Liu, and K. Maki, Phys. Rev. B **21**, 2388 (1980).
[19] T. Ishiguro, K. Yamaji, and G. Saito, *Organic Superconductors* (Springer, Berlin, 1998).
[20] P. G. de Gennes, *Superconductivity of Metals and Alloys*

(Addison-Wesley, Reading, MA, 1989).
[21] A. F. Andreev, Zh. Éksp. Teor. Fiz. **46**, 1823 (1964) [Sov. Phys. JETP **19**, 1228 (1964)].
[22] A. J. Leggett, Rev. Mod. Phys. **47**, 331 (1975).
[23] In the *g*-ology model (Ref. 19), the coupling constants g for singlet and triplet superconductivity are expressed in terms of forward- (g_2) and backward- (g_1) scattering amplitudes $g=g_2 \pm g_1$.
[24] The states (11) with $E_k<0$ are completely filled, whereas the state (9) with $E_0=0$ is half filled (Refs. 15 and 18).
[25] F. Schwabl, *Quantum Mechanics* (Springer, Berlin, 1995), Ch. 19; I. Adagideli, P. M. Goldbart, A. Shnirman, and A. Yazdani, Phys. Rev. Lett. **83**, 5571 (1999); I. Kosztin, Š. Kos, M. Stone, and A. J. Leggett, Phys. Rev. B **58**, 9365 (1998); G. Junker, *Supersymmetric Methods in Quantum and Statistical Physics* (Springer, Berlin, 1996).
[26] M. Stone, Ann. Phys. (N.Y.) **155**, 56 (1984).
[27] A. Yu. Kitaev, cond-mat/0010440 (unpublished).
[28] P. Coleman, A. J. Schofield, and A. M. Tsvelik, J. Phys.: Condens. Matter **8**, 9985 (1996).
[29] G. E. Blonder, M. Tinkham, and T. M. Klapwijk, Phys. Rev. B **25**, 4515 (1982).
[30] I. Žutić and O. T. Valls, Phys. Rev. B **60**, 6320 (1999); **61**, 1555 (2000).
[31] The $(TMTSF)_2X$ materials have high purity and the mean free path about 10 μ.
[32] I. Žutić and S. Das Sarma, Phys. Rev. B **60**, R16 322 (1999).
[33] The range of integration over $\mathbf{k}_\parallel$ in Eq. (13) may be limited by the acceptance cone of the tip.
[34] $a=\pi/2k_F$ is the crystal lattice period along the chains.
[35] The $d_{x^2-y^2}$ wave belongs to the same crystal symmetry class as the *s* wave, so it may be thought of as the extended *s* wave. That is why both of them do not show ZBCP. Similarly, the *f* wave proposed in Ref. 13 belongs to the same class as the p_x wave and has the same ZBCP.
[36] C.-R. Hu and X.-Z. Yan, Phys. Rev. B **60**, R12 573 (1999).
[37] The nonlinear Meissner effect can be also utilized to probe whether the superconducting pairing potential of $(TMTSF)_2X$ has nodes, see K. Halterman, O. T. Valls, and I. Žutić, Phys. Rev. B **63**, 014501 (2001).
[38] K. Sengupta, H.-J. Kwon, and V. M. Yakovenko, Phys. Rev. Lett. **86**, 1094 (2001).
[39] M. Covington *et al.*, Phys. Rev. Lett. **79**, 277 (1997); M. Fogelström, D. Rainer, and J. A. Sauls, *ibid.* **79**, 281 (1997).
[40] M. Fabrizio and A. O. Gogolin, Phys. Rev. B **51**, 17 827 (1995); A. O. Gogolin, *ibid.* **54**, 16 063 (1996); K. Le Hur, Europhys. Lett. **49**, 768 (2000).
[41] See D. A. Ivanov, cond-mat/9911147 (unpublished).